Journal of Cosmology and
Astroparticle Physics

PAPER

Monochromatic neutrinos from dark matter through the Higgs portal

Journal of Cosmology and Astroparticle Physics
An IOP and SISSA journal

Monochromatic neutrinos from dark matter through the Higgs portal

Pablo de la Torre, Miguel Gutiérrez and Manuel Masip

CAFPE and Departamento de Física Teórica y del Cosmos, Universidad de Granada, E-18071 Granada, Spain

E-mail: pdelatorre@ugr.es, mgg@ugr.es, masip@ugr.es

Received September 6, 2023
Accepted October 26, 2023
Published November 14, 2023

Abstract. We define a minimal model of dark matter with a fermion singlet χ coupled to the visible sector through the Higgs portal and with a heavy Dirac neutrino N that opens the annihilation channel $\chi\chi \to N\nu$. The model provides the observed relic abundance consistently with bounds from direct searches and implies a monochromatic neutrino signal at 10 GeV–1 TeV in indirect searches. In particular, we obtain the capture rate of χ by the Sun and show that the signal could be above the *neutrino floor* produced by cosmic rays showering in the solar surface. In most benchmark models this solar astrophysical background is above the expected dark matter signal, so the model that we propose is a canonical example of WIMP not excluded by direct searches that could be studied at neutrino telescopes and also at colliders.

Keywords: dark matter theory, dark matter experiments, neutrino astronomy

ArXiv ePrint: 2309.00374

https://doi.org/10.1088/1475-7516/2023/11/068

JCAP11(2023)068

Contents

1 Introduction

The WIMP paradigm provides arguably the simplest scenario for the dark matter (DM) of the universe. It represents a *smooth* extension of the Standard Model (SM), involving a physics that is new but that sounds quite familiar, not too exotic. The WIMP χ that constitutes the DM is stable just like the proton, with a matter parity playing the role of the baryon number. Its mass m_χ may introduce a new scale in physics, but this scale should not be far from the electroweak (EW) one. The same occurs with the mediators of its interactions with the visible sector: the EW gauge bosons do not work, but the Higgs boson may [1, 2] and, in any case, the interaction required should define EW-like cross sections. In the early universe the WIMP is in thermal equilibrium with the SM particles, until it decouples and its abundance freezes out just like happens to neutrinos, nothing extraordinary. This simplicity plus the fact that the scenario has interesting implications at direct, indirect and collider searches has made the WIMP the most popular DM candidate for over 40 years [3].

Indeed, WIMPs like the lightest odd particle in SUSY models with R-parity, in Little Higgs models with T-parity or in models with compact dimensions and KK-parity, are part of a setup that completes the SM at the TeV scale. The main motivation for these models was to solve the hierarchy problem, being the presence of a suitable DM candidate an interesting but additional feature. However, the LHC has basically discarded *naturality* as a guiding principle in the search for non-standard TeV physics. At this point it may be more effective an approach based on *minimality*, where one assumes that the new physics may appear with equal likelihood wherever it is not experimentally excluded. It is not that SUSY can not explain the DM, an anomaly in the muon $g-2$ or a peak followed by a dip in di-Higgs production at the LHC, it is that there is no need nor a strong motivation for the whole setup: keep just the few elements that are enough to explain the effect and save you the hustle of hiding the rest of the setup.

In that context, we will consider here a very minimal model of WIMP. The first basic question that such model should answer is whether it can provide the relic abundance $\Omega_c h^2 \approx$

JCAP11(2023)068

0.12 that we observe or, more precisely, if it can do it consistently with the bounds from direct searches. These searches push the WIMP-nucleon elastic cross section down, which tends to reduce the annihilation cross section and imply too large values of Ω_c. Second, it is interesting to know whether the model can be probed in indirect searches once the bounds from direct searches are imposed. Moreover, if these bounds reached the neutrino floor where the DM signal faces an (almost) irreducible background [4], could we still expect any positive results in indirect searches? We will focus on the signal from DM annihilation in the Sun at neutrino telescopes. On one hand, the same collisions with solar nuclei that capture the WIMP are also probed in direct searches. On the other hand, high energy cosmic rays (CRs) showering in the solar surface produce a flux of neutrinos [5–8] that, although not observed yet, represents a neutrino floor analogous to the one in direct search experiments [9].

The DM of the universe may involve physics at basically any scale. The thermal WIMP at $m_\chi = 10\,\text{GeV}$–$10\,\text{TeV}$ is just one of the many possibilities, but it is the only one that can be probed in direct, indirect and collider searches. Here we define a minimal setup that is consistent with the data in a wide range of parameters and that could imply an observable signal at neutrino telescopes and also at colliders. The model is a variation of the Higgs portal proposed a couple of decades ago [10–13] extended with a heavy Dirac neutrino. Due to its simplicity, it may help us to calibrate how constrained the WIMP paradigm currently is and what may be the chances to get a signal in future searches.

2 The model

Let us use 2-component spinors of left handed chirality to define the model.[1] We take χ as a Majorana singlet, although the results would be similar if the DM particle is a Dirac fermion. In addition, we introduce a Dirac singlet (N, N^c) of similar mass m_N; these fields are needed to make the SM neutrinos massive through an inverse see-saw (we assume that the rest of them are heavier and/or less coupled to the active neutrinos). We then assign odd matter parity to χ and $+1$ (-1) lepton number to N (N^c). If we consider an effective theory valid at energies below Λ, the relevant part of the Lagrangian is just

$$\begin{aligned} -\mathcal{L} \supset\; & \frac{1}{2}\, m_\chi\, \chi\chi + \frac{c_s}{\Lambda}\, H^\dagger H\, \chi\chi + i\, \frac{c_a}{\Lambda}\, H^\dagger H\, \chi\chi + \; m_N\, N N^c \\ & + \; y_N\, H L N^c + i\, \frac{c_N}{\Lambda^2} \left(N N^c + \bar{N}\bar{N}^c \right) (\chi\chi) + \text{h.c.}\,, \end{aligned} \tag{2.1}$$

where $H = (h^+\ h^0)$ is the SM Higgs, $L = (\nu\ \ell)$ a lepton doublet assumed mostly along the τ flavor, and the six parameters defining the model are real. Other possible terms, like the dim-5 operator $H^\dagger H\, N N^c$, give subleading effects that we will comment later on. Notice that in 4-spinor notation (see the footnote) the two operators connecting χ with H plus their conjugate are just $(c_s/\Lambda)\, H^\dagger H\, \bar{\Psi}_\chi \Psi_\chi - (i c_a/\Lambda)\, H^\dagger H\, \bar{\Psi}_\chi \gamma_5 \Psi_\chi$, whereas the dim-6 operator would read $(-i c_N/\Lambda^2)\, (\bar{\Psi}_N \Psi_N)(\bar{\Psi}_\chi \gamma_5 \Psi_\chi)$. These operators may result after integrating out heavy particles, in particular,

- A real scalar singlet s even under the matter parity coupled to the Higgs through the trilinear $sH^\dagger H$, to χ through the Yukawa $s\chi\chi$ (the real and imaginary parts of this

[1] In this 2-component notation e_α and e^c_α are the electron and the positron both *left*, whereas their conjugate-contravariant $\bar{e}^{\,\dot\alpha}$ and $\bar{e^c}^{\dot\alpha}$ are *right* spinors. The 4-component electron in the chiral representation of γ^μ is then $\Psi_e = \begin{pmatrix} e_\alpha \\ \bar{e^c}^{\dot\alpha} \end{pmatrix}$ [with $\bar{\Psi}_e = (e^{c\,\alpha}\ \bar{e}_{\dot\alpha})$], while $\Psi_\chi = \begin{pmatrix} \chi_\alpha \\ \bar{\chi}^{\dot\alpha} \end{pmatrix}$ is a Majorana fermion.

JCAP11(2023)068

coupling would contribute, respectively, to c_s and c_a) and to the heavy neutrino through sNN^c.

- A vectorlike lepton doublet (D, D^c) odd under the matter parity coupled to $HD\chi$ and $H^\dagger D^c\chi$ may generate values of c_s and c_a that will depend on the relative complex phase in these two Yukawas.

Notice also that in the first case the SM Higgs will necessarily mix with s and the mass eigenstate will get a small singlet component, whereas in the second model it is the fermion singlet χ who will mix with the neutral fermions in (D, D^c) and acquire a small doublet component. This could introduce interesting effects in the UV complete model, but they are subleading in the regime that we assume with s and (D, D^c) heavier than χ and N.

Let us then continue with the effective model. At the EW minimum, $\langle H\rangle = (0\ v/\sqrt{2})$, in the unitary gauge the Lagrangian includes (we use primes to denote mass eigenstates)

$$
\begin{aligned}
-\mathcal{L} \supset\ & \frac{1}{2}\, m'_\chi\, \chi\chi + m'_N\, N' N^c + \frac{\tilde{y}_N}{\sqrt{2}}\, h\, \nu' N^c + \frac{c_s + i c_a}{2\Lambda}\, (hh\, \chi\chi + 2h\, \chi\chi) \\
& + \frac{i c_N}{\Lambda^2}\, (c_\alpha\, N' N^c + s_\alpha\, \nu' N^c + c_\alpha\, \bar{N}' \bar{N}^c + s_\alpha\, \bar{\nu}' \bar{N}^c)\, (\chi\chi) + \text{h.c.}\,,
\end{aligned} \tag{2.2}
$$

where $N' = c_\alpha\, N + s_\alpha\, \nu$ and N^c combine into a heavy Dirac neutrino of mass

$$
m'_N = \sqrt{\left(\frac{y_N v}{\sqrt{2}}\right)^2 + m_N^2} \tag{2.3}
$$

while the orthogonal combination $\nu' = c_\alpha\, \nu - s_\alpha\, N$ remains massless. The active-sterile mixing is just $s_\alpha = \frac{y_N v}{\sqrt{2}\, m'_N}$, whereas the Yukawa coupling $\tilde{y}_N$,

$$
\tilde{y}_N = y_N\, c_\alpha = \frac{\sqrt{2}\, m'_N}{v}\, c_\alpha\, s_\alpha \tag{2.4}
$$

may receive a contribution from the dim-5 operator $H^\dagger H\, N N^c$ that could be sizeable for $m'_N \lesssim v$. The mass of ν' and of the other two SM neutrinos should then be implemented through an inverse see-saw mechanism. A particular model along these lines has been recently proposed as a solution to the so called H_0 tension [14, 15].

In summary, the setup includes 6 parameters (we drop all the primes): the mass m_χ of the DM particle; the two couplings $c_{s,a}/\Lambda$ connecting χ with the Higgs; the mass m_N of a heavy Dirac neutrino (N, N^c); the heavy-light Yukawa $\tilde{y}_N$ (correlated with the mixing s_α), and the coupling c_N/Λ^2 connecting χ with the heavy neutrino.

3 Cross sections

We are interested in the production of monochromatic neutrinos through $\chi\chi \to N\nu$ (we use $N\nu$ to indicate $\bar{N}\nu + N\bar{\nu}$, see the two relevant diagrams in figure 1), so we will consider relatively large values of the coupling $\tilde{y}_N$ and of the four fermion coefficient c_N. In particular, notice that the Yukawa $\tilde{y}_N$ does not imply a mass for the active neutrino, it is just constrained by collider bounds on the heavy-light mixing (assumed mostly along the tau flavor), $s_\alpha \leq 0.1$ [16–18]. Since $s_\alpha = m_N/(174\ \text{GeV})$, only values of m_N above 1 TeV will allow for top-like Yukawa couplings. In any case, to avoid LEP bounds from $Z \to N\nu$ plus $N \to \tau W^*, \nu Z^*$ we

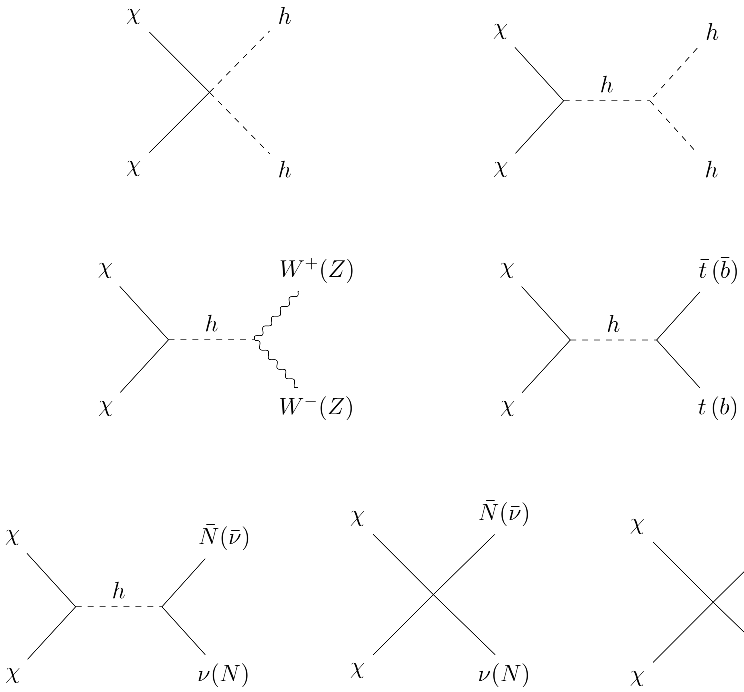

Figure 1. Leading diagrams in DM annihilation.

will not consider values of m_N below M_Z. In turn, if the annihilation channel $\chi\chi \to N\nu$ is open this implies that $m_\chi > M_Z/2$. Throughout the analysis we will then take $m_\chi \geq 50\,\mathrm{GeV}$, $m_N \geq 100\,\mathrm{GeV}$, $s_\alpha = 0.1$ and $c_i/\Lambda < 1/(2m\chi), 1/v$.

The DM annihilation in the early universe and in astrophysical environments will go through the diagrams in figure 1. If we neglect c_N (the last two diagrams in the figure) the cross section can be written

$$\sigma_{\mathrm{ann}}^{(1)} = \frac{c_s^2\left(1-\frac{4m_\chi^2}{s}\right)+c_a^2}{4\pi\Lambda^2\left(1-\frac{4m_\chi^2}{s}\right)^{1/2}}\, f(m_\chi) \approx \frac{c_s^2\,\beta^2+c_a^2}{4\pi\Lambda^2\,\beta}\, f(m_\chi)\,, \tag{3.1}$$

where β is the velocity of χ in the center of mass frame and $f(m_\chi) = \sum_i f_i$ gives the contribution of the different channels for a given value of m_χ. We obtain

$$\begin{aligned}
f_{hh} &= \left(1+\frac{3m_h^2}{s-m_h^2}\right)\sqrt{1-\frac{4m_h^2}{s}} \\
f_{QQ} &= \frac{3m_Q^2\left(s-4m_Q^2\right)}{\left(s-m_h^2\right)^2}\sqrt{1-\frac{4m_Q^2}{s}} \\
f_{VV} &= \frac{2m_V^4}{\left(s-m_h\right)^2}\left[2+\left(1-\frac{s}{2m_V^2}\right)^2\right]\sqrt{1-\frac{4m_V^2}{s}} \\
f_{N\nu}^{(1)} &= \frac{\tilde{y}_N^2 v^2\left(s-m_N^2\right)}{2\left(s-m_h^2\right)^2}\left(1-\frac{m_N^2}{s}\right)
\end{aligned} \tag{3.2}$$

JCAP11(2023)068

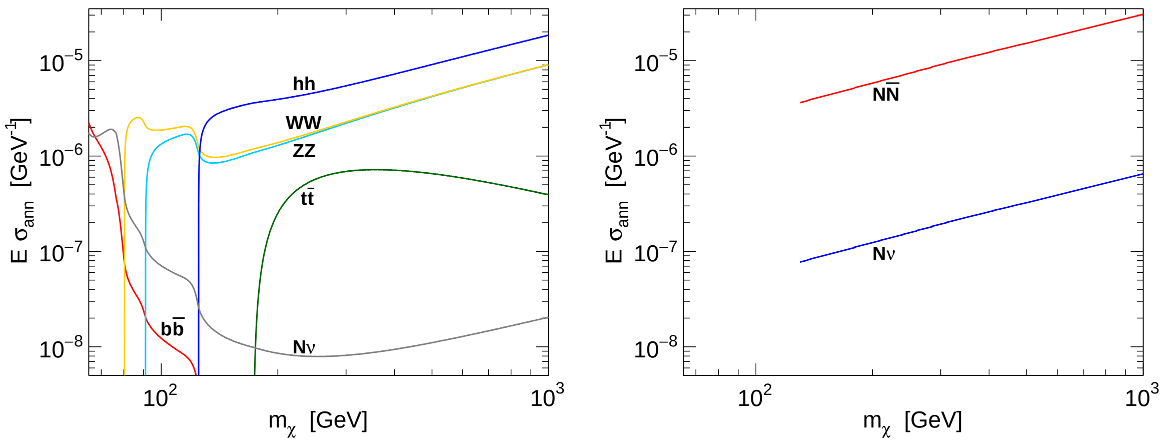

Figure 2. Different contributions to $\sigma_{\rm ann}$ for $c_N \to 0$, $m_N = 1.4\, m_\chi$ (left) and $c_a \to 0$, $m_N = 0.7\, m_\chi$ (right). We have taken $s_\alpha = 0.1$ and $\beta = 1/20$.

with $Q = t, b$ and $V = Z, W$. If c_N is sizeable we have to add

$$\sigma^{(2)}_{\rm ann} = \frac{c_N^2}{4\pi\Lambda^2 \left(1 - \frac{4m_\chi^2}{s}\right)^{1/2}} \left(f_{NN} + f^{(2)}_{N\nu}\right) , \tag{3.3}$$

where

$$\begin{aligned} f_{NN} &= \frac{c_\alpha^2 \left(s - 4m_N^2\right)}{\Lambda^2} \sqrt{1 - \frac{4m_N^2}{s}} \\ f^{(2)}_{N\nu} &= \left(\frac{s_\alpha^2}{\Lambda^2} - \frac{\sqrt{2}\, c_a\, \tilde{y}_N v}{c_N \Lambda \left(s - m_h^2\right)}\right) \left(s - m_N^2\right) \left(1 - \frac{m_N^2}{s}\right) . \end{aligned} \tag{3.4}$$

Notice that at $s \approx 4m_\chi^2$ the channel $\chi\chi \to N\nu$ produces an active neutrino of energy

$$E_\nu = m_\chi \left(1 - \frac{m_N^2}{4m_\chi^2}\right) . \tag{3.5}$$

In figure 2 we plot the contribution of the different channels for values of m_χ between 65 GeV and 1 TeV in the limits $c_N \to 0$ and $c_a \to 0$. Whenever $m_N < m_h$ and the Higgs can decay $h \to N\nu$, we use the value of y_N implying a 10% branching ratio for this channel (see discussion in section 5.1). In all the cases we have $m_N > M_{W,Z}$.

The second relevant cross section is the one describing the elastic scattering of χ with a nucleon $\mathcal{N}$, which is mediated by a Higgs in the t channel. The Higgs boson couples to the quarks and (through heavy quark loops) to the gluons in the nucleon; at low energies this induces a Higgs-nucleon Yukawa coupling $g_{h\mathcal{N}}$ that is usually parametrized as $g_{h\mathcal{N}} = f_\mathcal{N} m_\mathcal{N}/v$ [19, 20], with $m_\mathcal{N} = 0.94$ GeV and $f_\mathcal{N} = 0.30$ [21, 22]. We obtain

$$\sigma(\chi\mathcal{N} \to \chi\mathcal{N}) = \frac{4}{\pi} \frac{c_s^2 + c_a^2\, \beta^2}{\Lambda^2} \left(\frac{\mu_\mathcal{N}\, m_\mathcal{N} f_\mathcal{N}}{m_h^2}\right)^2 , \tag{3.6}$$

with $\mu_\mathcal{N} = m_\mathcal{N} m_\chi/(m_\mathcal{N} + m_\chi)$.

JCAP11(2023)068

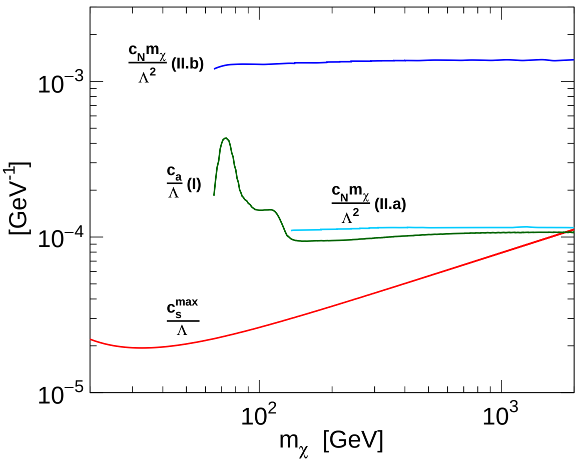

Figure 3. Maximum coupling c_s/Λ allowed by direct searches together with the value of c_a/Λ (case I) or $c_N m_\chi/\Lambda^2$ with $m_N = 0.7\, m_\chi$ (case II.a) and $1.4\, m_\chi$ (II.b) implying $\Omega_c h^2 = 0.12$.

4 Direct searches and relic abundance

Direct searches expect to see the recoil of a nucleus hit by a DM particle of velocity $\beta \approx 10^{-3}$. Therefore, these experiments do not constrain significantly the coupling c_a in eq. (3.6), whose contribution to the cross section is suppressed by a factor of β^2, nor c_N, that couples χ only to neutrinos. In contrast, the coupling c_s implies an unsuppressed spin-independent cross section that must respect the XENON1T bounds [23]. For m_χ between 10 GeV and 10 TeV we fit these bounds to

$$\sigma^{\rm SI}_{\chi\mathcal{N}} \lesssim 0.9 \times 10^{-48}\, m_\chi^{1+169/m_\chi^2}\ {\rm cm}^2, \tag{4.1}$$

with m_χ in GeV. This implies

$$\frac{c_s}{\Lambda} \leq \frac{c_s^{\max}}{\Lambda} \approx 2.5 \times 10^{-6}\, \frac{0.94 + m_\chi}{\sqrt{m_\chi^{1-169/m_\chi^2}}}\ {\rm GeV}^{-1}. \tag{4.2}$$

On the other hand, in $\sigma_{\rm ann}$ (see eq. (3.1)) it is the contribution of c_s the one suppressed by a factor of β^2, with $\beta \approx 1/20$ during freeze out, and c_a and/or c_N should provide the dominant contribution. It is straightforward to find the values of these couplings implying a relic abundance $\Omega_c h^2 \approx 0.12$ for each value of m_χ. We distinguish the two cases that we plot in figure 3:

I. If $c_N \to 0$ there is a value of c_a/Λ giving $\Omega_c h^2 \approx 0.12$. Notice that the channel $\chi\chi \to N\nu$ is in this case subleading and thus the dependence of c_a/Λ on m_N can be neglected (in the plot we use $m_N = 1.4\, m_\chi$).

II. If $c_a \to 0$ there is also a value of c_N/Λ^2 giving the right relic abundance. Here, however, we have to distinguish two possibilities: $m_N < m_\chi$, so that the channel $\chi\bar{\chi} \to N\bar{N}$ is open (we take $m_N = 0.7 m_\chi$), or $m_N > m_\chi$ and a DM particle that annihilates predominantly into $N\nu$, as the contribution to $\sigma_{\rm ann}$ of the rest of channels is proportional to $c_s^2 \beta^2$.

JCAP11(2023)068

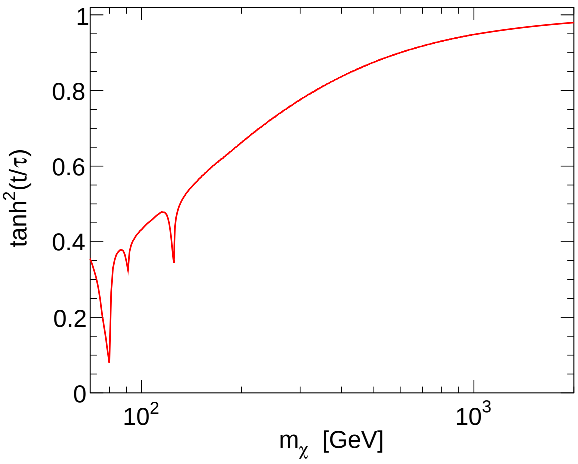

Figure 4. Suppression factor $\tanh^2(t_\odot/\tau)$ for different values of m_χ.

The general model will combine both cases with weights $\omega_a = c_a^2/\tilde{c}_a^2$ and $\omega_N = c_N^2/\tilde{c}_N^2$, where $\tilde{c}_a$ and $\tilde{c}_N$ are the values of the couplings in the two limiting cases.

5 Indirect searches at neutrino telescopes

We will finally consider the possible signal implied by this model at neutrino telescopes. In particular, we will study whether the signal from DM annihilation in the Sun may be above the background produced by CRs showering in the solar surface [5–9] (in the appendix we provide an approximate fit for this CR background). As the capture rate $C = \mathrm{d}N_\chi^{\mathrm{cap}}/\mathrm{d}t$ of DM by the Sun depends on the same elastic cross section probed at direct searches, we will consider the maximum coupling $c_s^{\max}/\Lambda$ consistent with the bounds from XENON1T.

In our estimate of C we will take the spin-independent DM-nucleon cross section in eq. (3.6), neglecting the velocity-dependent contribution proportional to $\beta^2 \approx 10^{-6}$. To deduce the elastic cross section with the different solar nuclei we use the nuclear response functions in [24]. In particular, we include the collisions with the 6 most abundant nuclei in the Sun (H, He, N, O, Ne, Fe). We will assume the AGSS09 solar model [25] and the SHM^{++} velocity distribution of the galactic DM [26]. Our calculation also includes the thermal velocity of the solar nuclei, although its net effect is not important (e.g., at $m_\chi = 100\,\mathrm{GeV}$ it increases a 5% the capture rate by solar hydrogen but reduces in a 40% the one by iron, and both effects cancel). For $m_\chi \geq 10\,\mathrm{GeV}$ and a maximum coupling $c_s^{\max}/\Lambda$ we obtain a capture rate that can be fit to

$$C^{\max} \approx 2.30 \times 10^{21}\, m_\chi^{-1-\frac{22}{m_\chi}+\frac{240}{m_\chi^2}}\ \mathrm{s}^{-1}, \tag{5.1}$$

with m_χ expressed in GeV.

Although in our model the annihilation cross section required to reproduce the relic abundance is relatively large, we need to check whether the age $t_\odot \approx 4.5$ Gyr of the Sun is long enough to achieve the stationary state where the annihilation rate Γ_A is half the capture rate, $\Gamma_A = C/2$. In particular, if we express $\Gamma_A \equiv \frac{1}{2} C_A N_\chi^2$ [27] the time scale τ for capture

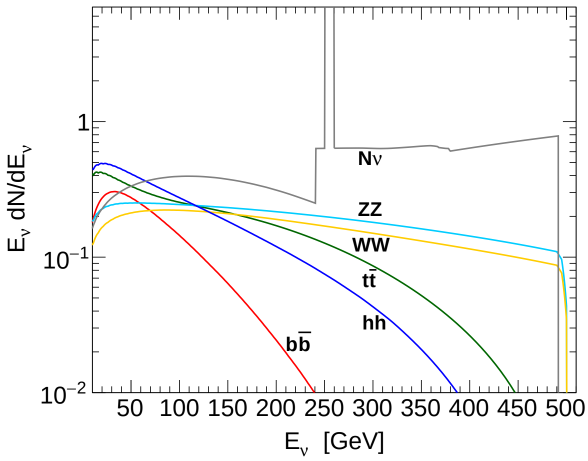

Figure 5. Neutrino yield per one annihilation through each channel for $m_\chi = 500\,\mathrm{GeV}$, $m_N = 700\,\mathrm{GeV}$.

and annihilation to equilibrate is just $\tau = (CC_A)^{-1/2}$, and [28]

$$\frac{t_\odot}{\tau} \approx 330 \left(\frac{C}{\mathrm{s}^{-1}}\right)^{1/2} \left(\frac{\langle\sigma_{\mathrm{ann}}\beta\rangle}{\mathrm{cm}^3\,\mathrm{s}^{-1}}\right)^{1/2} \left(\frac{m_\chi}{10\,\mathrm{GeV}}\right)^{3/4}. \tag{5.2}$$

If $t_\odot/\tau \gg 1$ then $\Gamma_A \approx C/2$, otherwise the annihilation rate is suppressed to

$$\Gamma_A = \frac{C}{2}\tanh^2\frac{t_\odot}{\tau}. \tag{5.3}$$

In figure 4 we show that, even for the maximum capture rate allowed by bounds from direct searches, this suppression cannot be ignored, specially for low values of m_X.

As for the neutrino yields after propagation from the Sun to the Earth, we use the Monte Carlo simulator CHARON [29]. In figure 5 we plot the total neutrino yield (ν and $\bar{\nu}$ of all flavors) per annihilation through each channel for $m_\chi = 500\,\mathrm{GeV}$ and $m_N = 1.4\,m_\chi$. Let us illustrate our results by discussing in some detail a couple of cases.

5.1 $m_\chi = 300\,\mathrm{GeV}$, $m_N = 105\,\mathrm{GeV}$

We have imposed $m_N > m_Z$ to reduce the decays of weak bosons into the heavy neutrino ($Z \to N\nu$, $W \to N\ell$, being ℓ most frequently the τ lepton), but we will consider the possibility that N is produced in Higgs decays ($h \to N\nu$) as long as the branching ratio is below 10%. At the LHC an event with the Higgs giving a heavy neutrino that decays $N \to \ell W$ would appear as a small correction to $h \to W^*W$ plus $W^* \to \nu\ell$ (a process still unobserved for $\ell = \tau$) [30, 31], whereas the 10% increase in the total Higgs width introduced by the new channel is not experimentally excluded. An analogous argument would apply to $h \to N\nu$ with $N \to Z\nu$, which would correct $h \to Z^*Z$ plus one (or both [32]) of the Z bosons decaying into neutrinos [33].

Therefore, we consider the case with $m_\chi = 300\,\mathrm{GeV}$, $m_N = 105\,\mathrm{GeV}$, and a Yukawa $\tilde{y}_N = 0.11$ implying $\mathrm{BR}(h \to N\nu) = 0.1$. We set the maximum coupling consistent with direct bounds, $c_s^{\max}/\Lambda = 4.37 \times 10^{-5}\,\mathrm{GeV}^{-1}$, and we choose for c_a/Λ and c_N/Λ^2 the values

JCAP11(2023)068

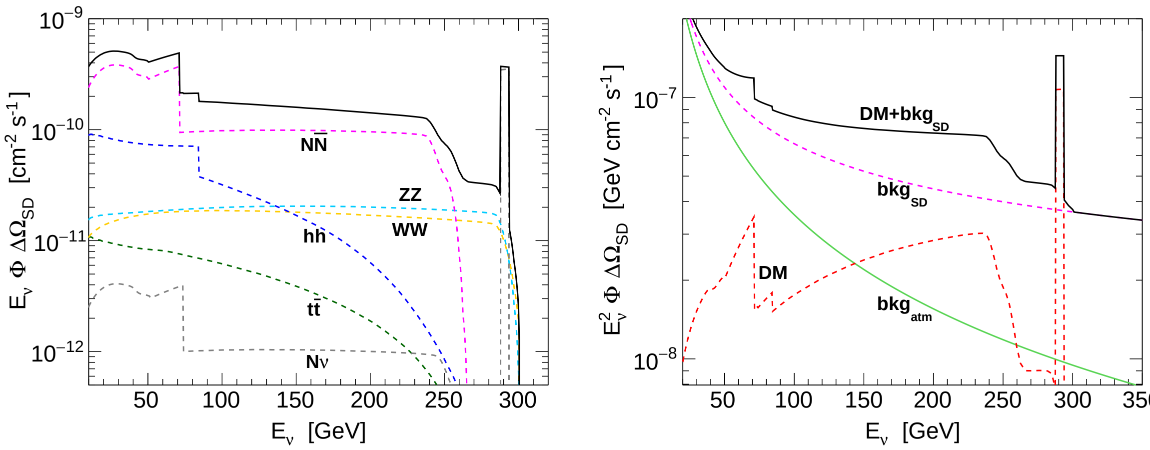

Figure 6. Solar neutrino flux for $m_\chi = 300\,\mathrm{GeV}$, $m_N = 105\,\mathrm{GeV}$, $\omega_a = 0.5 = \omega_N$. On the left, the contribution of the different annihilations channels; on the right, total flux from the SD including the CR background (for comparison, we include the atmospheric flux from a *fake* Sun). The bin containing the monochromatic ν's has a width of 6 GeV.

giving $\omega_a = 0.5 = \omega_N$, i.e., DM annihilates with equal frequency to $(N\bar{N}, N\bar{\nu}, \bar{N}\nu)$ or through the channels in figure 2-left.

At this value of m_χ and m_N the dominant annihilation channels are into heavy neutrino and Higgs boson pairs. The neutrinos ν from $\chi\chi \to hh$ plus $h \to N\nu$ are not monochromatic, their energy is distributed between

$$E_\nu^{\min} = \frac{1}{2}\left(m_\chi - \sqrt{m_\chi^2 - m_h^2} - \frac{m_N^2}{m_\chi + \sqrt{m_\chi^2 - m_h^2}} \right) \tag{5.4}$$

and

$$E_\nu^{\max} = \frac{1}{2}\left(m_\chi + \sqrt{m_\chi^2 - m_h^2} - \frac{m_N^2}{m_\chi - \sqrt{m_\chi^2 - m_h^2}} \right) . \tag{5.5}$$

However, when m_χ in near m_h the energy interval shrinks (in the case at hand it goes from 4 GeV to 84 GeV). The monocromatic channel $\chi\chi \to N\nu$ gives $E_\nu = 290\,\mathrm{GeV}$.

In figure 6-left we plot the contribution of each annihilation channel to the neutrino flux from DM annihilation in the Sun. On the right, we plot the total flux from the solar disk (SD) including both the DM contribution and the neutrino background produced by CR showers in the Sun and by the partial shadow of the Sun (see appendix) for $\theta_z = 45°$. For comparison, we have also included the atmospheric flux from a *fake* Sun at the same zenith angle.

5.2 $m_\chi = 1\,\mathrm{TeV}$, $m_N = 1.4\,\mathrm{TeV}$

At these values of m_χ and m_N all annihilation channels into standard particles are open but $\chi\chi \to N\bar{N}$ is closed. We take the maximum value of c_s/Λ consistent with direct bounds and assume that the channels in figure 2-left contribute a 50% to σ_{ann}, with $\chi\chi \to N\nu$ providing the rest. In this case Higgs decays are unaffected by the heavy neutrino, that may only appear in flavor analyses [16–18].

JCAP11(2023)068

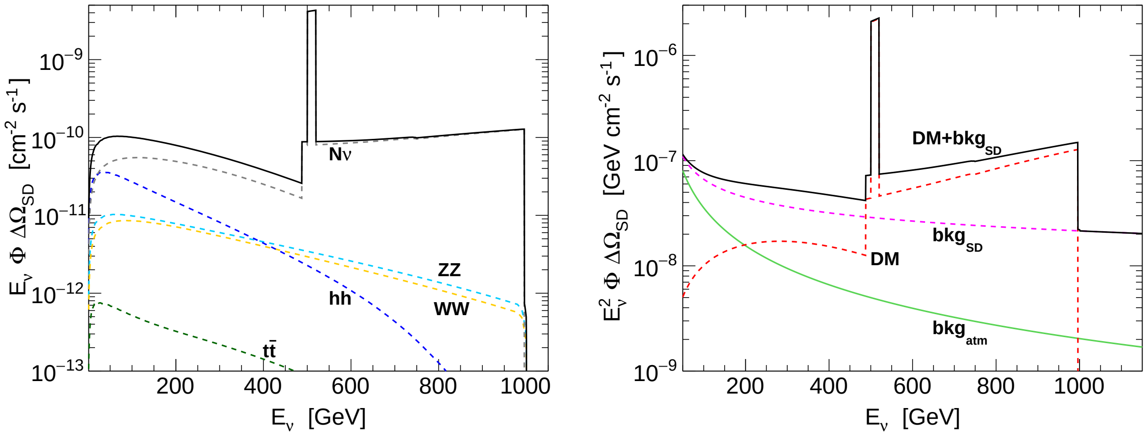

Figure 7. Neutrino flux from the SD for $m_\chi = 1\,\text{TeV}$, $m_N = 1.4\,\text{TeV}$, $\omega_a = 0.5 = \omega_N$. On the left, contribution of the different annihilations channels; on the right, total flux including the CR background. The bin containing the monochromatic ν's has a width of 20 GeV.

We find a DM signal (see figure 7) that is clearly above the CR background from the solar disk: 2.28 neutrinos per km^2 and second at 500–1000 GeV from DM annihilation (1.62 of them at the 500-520 GeV energy bin), and only 0.25 neutrinos from CRs showers in the solar surface or from the partial CR shadow of the Sun. The atmospheric background from a fake Sun at the same zenith inclination would account for just 0.03 km^{-2} s^{-1} in the same energy interval.

6 Summary and discussion

The WIMP paradigm has been studied for decades, and currently a variety of experiments severely constrains the different models. In particular, the absence of a signal in direct searches and of missing E_T at colliders discard the Z and W gauge bosons as viable mediators of its interactions with the visible sector, as suggested by the so called WIMP miracle. The Higgs portal appears then as an equally minimal and appealing possibility. Although the Higgs boson has stronger couplings to the heavier SM particles (i.e., to itself, the top quark and the weak gauge bosons), it also admits large Yukawa couplings with the active neutrinos in the presence of heavy Dirac neutral fermions. Those couplings would introduce heavy-light mixings and are actually expected if the origin of neutrino masses is an inverse seesaw mechanism at the TeV scale.

In this work we have analysed such a WIMP scenario: a Majorana fermion interacting through the Higgs portal in a model extended with a heavy Dirac neutrino. First we show that, although the WIMP interactions are all spin independent and are thus severely constrained by direct searches, the model naturally implies the observed relic abundance while respecting the current bounds. The question is then whether such a constrained model may provide *any* signal in indirect or collider searches at all.

For the neutrino signal from DM annihilation in the Sun, in particular, the same spin independent elastic cross section probed in direct searches also dictates the capture rate by the Sun. In addition, CRs reaching the solar surface produce an irreducible neutrino background that defines a floor in DM searches. It has been shown that a capture rate consistent with the current XENON1T bounds implies a neutrino flux from DM annihilations into $\tau^+\tau^-$,

$b\bar{b}$ or W^+W^- already below this floor [9], i.e., these WIMPs should not give any observable signal there.

The model proposed here, however, is *neutrinophilic*. Most important, it includes an annihilation channel $\chi\chi \to \nu N$ that produces a monochromatic neutrino signal that could be probed at telescopes [34]. The search there for the astrophysical signal from CRs showering in the solar surface may then also reveal this type of DM signal.

The scenario could have interesting implications at the LHC as well [13, 35], especially if the heavy neutrino in the model is lighter than the Higgs boson. The decays $h \to N\nu$ with $N \to \ell W$ (with ℓ most frequently the τ lepton but also the lighter flavors) or $N \to \nu Z$ would appear as a non-standard contribution in $h \to WW^*, ZZ^*$ searches, where 10% deviations from the SM prediction are not yet experimentally excluded.

In summary, although the WIMP is a DM candidate certainly constrained by several decades of experimental searches, we think that the presence of heavy Dirac neutrinos at the TeV scale revives all the reasons why the scenario is phenomenologically interesting.

Acknowledgments

We would like to thank Miki R. Chala, Pablo Olgoso and José Santiago for discussions. This work was partially supported by the Spanish Ministry of Science, Innovation and Universities (PID2019-107844GB-C21/AEI/10.13039/501100011033) and by the Junta de Andalucía (FQM 101).

A Cosmic ray background

Here we provide approximate fits for the atmospheric and solar neutrino fluxes of CR origin that are a background in DM searches. To obtain these fluxes we have followed the procedure in [9], setting the parameter E_c to 5 TeV (versus 3–6 TeV in that reference) in order to obtain an optimal fit of recent HAWC data on the gamma-ray flux at 1 TeV [36]. In figure 7 we include that flux together with the model prediction.

In the expressions below we give the neutrino flux integrated over the angular region ($\Delta\Omega_\odot$) occupied by the Sun, with E is in GeV, t in years ($t = 0$ at the solar minimum), and $\Delta\Omega_\odot\, \Phi_\nu$ in GeV^{-1} cm^{-2} s^{-1}. The angle $\theta^*(\theta_z)$ is defined in [38, 39]:

$$\tan\theta^* = \frac{R_\oplus \sin\theta_z}{\sqrt{R_\oplus^2 \cos^2\theta_z + (2R_\oplus + h)\, h}}\,. \tag{A.1}$$

For the atmospheric flux we have

$$\Delta\Omega_\odot\, \Phi_{\nu_\mu}^{\rm atm}(E,\theta) = 4.41 \times 10^{-6}\; E^{-2.97-0.0109\log E-0.00139\log^2 E}\; F_1^{\rm atm}(E,\theta)\,; \tag{A.2}$$

$$\Delta\Omega_\odot\, \Phi_{\nu_e}^{\rm atm}(E,\theta) = 1.94 \times 10^{-6}\; E^{-3.30-0.0364\log^{1.35} E+0.0103\log^{1.85} E}\; F_2^{\rm atm}(E,\theta) \tag{A.3}$$

with

$$F_1^{\rm atm}(E,\theta) = \frac{\left(\frac{176}{E}\right)^{0.6} + \cos[\theta^*(\frac{\pi}{4})]}{\left(\frac{176}{E}\right)^{0.6} + \cos[\theta^*(\theta_z)]}\,;\quad F_2^{\rm atm}(E,\theta) = \frac{\left(\frac{7.5\times 10^{-4}}{E}\right)^{0.21} + \cos[\theta^*(\frac{\pi}{4})]}{\left(\frac{7.5\times 10^{-4}}{E}\right)^{0.21} + \cos[\theta^*(\theta_z)]}\,. \tag{A.4}$$

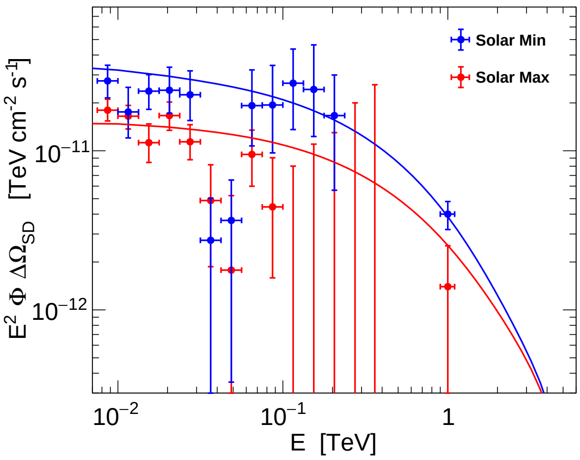

Figure 8. Gamma-ray flux from the solar disk obtained with the model in [9] for $E_c = 5\,\text{TeV}$ and data from HAWC ($E = 1\,\text{TeV}$) [36] and Fermi-LAT (at $E \leq 200\,\text{GeV}$) [37].

For the atmospheric neutrinos from the partial cosmic ray shadow of the Sun and from neutrons produced in the solar surface and reaching the Earth the flux is

$$\Delta\Omega_\odot\, \Phi^{\text{shad+n}}_{\nu_\mu}(E,\theta,t) = 4.33\times 10^{-6}\ E^{G_1^{\text{atm}}(E,t)}\, F_2^{\text{atm}}(E,\theta)\,; \tag{A.5}$$

$$\Delta\Omega_\odot\, \Phi^{\text{shad+n}}_{\nu_e}(E,\theta,t) = 1.37\times 10^{-6}\ E^{G_2^{\text{shad+n}}(E,t)}\, F_2^{\text{atm}}(E,\theta) \tag{A.6}$$

with

$$G_1^{\text{shad+n}}(E,t) = -2.98 - 0.017\log E + 0.012\cos\frac{2\pi t}{11}\log^2 E - 3.3\times 10^{-4}\log^3 E \\ - 3.9\times 10^{-6}\log^5 E\,; \tag{A.7}$$

$$G_2^{\text{shad+n}}(E,t) = -3.1 - 0.061\log E - \cos\frac{2\pi t}{11}\left(0.00305\log E + 2.1\times 10^{-6}\log^5 E\right) \\ - 5.4\times 10^{-7}\log^6 E\,. \tag{A.8}$$

Finally, the neutrinos produced by cosmic rays in the Sun reach us in the three flavors with the same frequency and a flux per flavor

$$\Delta\Omega_\odot\, \Phi^{\odot}_{\nu_i}(E,t) = 6.0\times 10^{-9}\left(1 - \frac{405\sin^2\frac{\pi t}{11}}{900+E}\right) E^{-1.20-0.1\log E-0.0042\log^2 E+1.6\times 10^{-5}\log^4 E}\,. \tag{A.9}$$

References

[1] O. Lebedev, *The Higgs portal to cosmology*, *Prog. Part. Nucl. Phys.* **120** (2021) 103881 [arXiv:2104.03342] [INSPIRE].

[2] G. Arcadi, A. Djouadi and M. Kado, *The Higgs-portal for dark matter: effective field theories versus concrete realizations*, *Eur. Phys. J. C* **81** (2021) 653 [arXiv:2101.02507] [INSPIRE].

[3] M.S. Turner, *Cosmology and particle physics*, *Conf. Proc. C* **831228** (1983) 99 [INSPIRE].

[4] C.A.J. O'Hare, *New definition of the neutrino floor for direct dark matter searches*, *Phys. Rev. Lett.* **127** (2021) 251802 [arXiv:2109.03116] [INSPIRE].

[5] D. Seckel, T. Stanev and T.K. Gaisser, *Signatures of cosmic-ray interactions on the solar surface*, *Astrophys. J.* **382** (1991) 652 [INSPIRE].

[6] J. Edsjo, J. Elevant, R. Enberg and C. Niblaeus, *Neutrinos from cosmic ray interactions in the sun*, *JCAP* **06** (2017) 033 [arXiv:1704.02892] [INSPIRE].

[7] M. Masip, *High energy neutrinos from the sun*, *Astropart. Phys.* **97** (2018) 63 [arXiv:1706.01290] [INSPIRE].

[8] M. Gutiérrez and M. Masip, *The sun at TeV energies: gammas, neutrons, neutrinos and a cosmic ray shadow*, *Astropart. Phys.* **119** (2020) 102440 [arXiv:1911.07530] [INSPIRE].

[9] M. Gutiérrez, M. Masip and S. Muñoz, *The solar disk at high energies*, *Astrophys. J.* **941** (2022) 86 [arXiv:2206.00964] [INSPIRE].

[10] Y.G. Kim and K.Y. Lee, *The minimal model of fermionic dark matter*, *Phys. Rev. D* **75** (2007) 115012 [hep-ph/0611069] [INSPIRE].

[11] L. Lopez-Honorez, T. Schwetz and J. Zupan, *Higgs portal, fermionic dark matter, and a Standard Model like Higgs at* 125 *GeV*, *Phys. Lett. B* **716** (2012) 179 [arXiv:1203.2064] [INSPIRE].

[12] S. Baek, P. Ko and W.-I. Park, *Search for the Higgs portal to a singlet fermionic dark matter at the LHC*, *JHEP* **02** (2012) 047 [arXiv:1112.1847] [INSPIRE].

[13] A. Djouadi, O. Lebedev, Y. Mambrini and J. Quevillon, *Implications of LHC searches for Higgs-portal dark matter*, *Phys. Lett. B* **709** (2012) 65 [arXiv:1112.3299] [INSPIRE].

[14] A.J. Cuesta, M.E. Gómez, J.I. Illana and M. Masip, *Cosmology of an axion-like majoron*, *JCAP* **04** (2022) 009 [arXiv:2109.07336] [INSPIRE].

[15] A.J. Cuesta, J.I. Illana and M. Masip, *Photon to axion conversion during big bang nucleosynthesis*, arXiv:2305.16838 [INSPIRE].

[16] G. Hernández-Tomé et al., *Effects of heavy Majorana neutrinos on lepton flavor violating processes*, *Phys. Rev. D* **101** (2020) 075020 [arXiv:1912.13327] [INSPIRE].

[17] G. Hernández-Tomé, J.I. Illana and M. Masip, *The ρ parameter and $H^0 \to \ell_i \ell_j$ in models with TeV sterile neutrinos*, *Phys. Rev. D* **102** (2020) 113006 [arXiv:2005.11234] [INSPIRE].

[18] E. Fernandez-Martinez, J. Hernandez-Garcia and J. Lopez-Pavon, *Global constraints on heavy neutrino mixing*, *JHEP* **08** (2016) 033 [arXiv:1605.08774] [INSPIRE].

[19] J.M. Cline, K. Kainulainen, P. Scott and C. Weniger, *Update on scalar singlet dark matter*, *Phys. Rev. D* **88** (2013) 055025 [*Erratum ibid.* **92** (2015) 039906] [arXiv:1306.4710] [INSPIRE].

[20] J.A. Casas, D.G. Cerdeño, J.M. Moreno and J. Quilis, *Reopening the Higgs portal for single scalar dark matter*, *JHEP* **05** (2017) 036 [arXiv:1701.08134] [INSPIRE].

[21] J.M. Alarcon, J. Martin Camalich and J.A. Oller, *The chiral representation of the πN scattering amplitude and the pion-nucleon sigma term*, *Phys. Rev. D* **85** (2012) 051503 [arXiv:1110.3797] [INSPIRE].

[22] ETM collaboration, *Direct evaluation of the quark content of nucleons from lattice QCD at the physical point*, *Phys. Rev. Lett.* **116** (2016) 252001 [arXiv:1601.01624] [INSPIRE].

[23] XENON collaboration, *Dark matter search results from a one ton-year exposure of XENON1T*, *Phys. Rev. Lett.* **121** (2018) 111302 [arXiv:1805.12562] [INSPIRE].

[24] R. Catena and B. Schwabe, *Form factors for dark matter capture by the sun in effective theories*, *JCAP* **04** (2015) 042 [arXiv:1501.03729] [INSPIRE].

JCAP11(2023)068

[25] M. Asplund, N. Grevesse, A.J. Sauval and P. Scott, *The chemical composition of the sun*, *Ann. Rev. Astron. Astrophys.* **47** (2009) 481 [arXiv:0909.0948] [INSPIRE].

[26] N.W. Evans, C.A.J. O'Hare and C. McCabe, *Refinement of the standard halo model for dark matter searches in light of the Gaia sausage*, *Phys. Rev. D* **99** (2019) 023012 [arXiv:1810.11468] [INSPIRE].

[27] K. Griest and D. Seckel, *Cosmic asymmetry, neutrinos and the sun*, *Nucl. Phys. B* **283** (1987) 681 [*Erratum ibid.* **296** (1988) 1034] [INSPIRE].

[28] G. Jungman, M. Kamionkowski and K. Griest, *Supersymmetric dark matter*, *Phys. Rept.* **267** (1996) 195 [hep-ph/9506380] [INSPIRE].

[29] Q. Liu et al., *Charon: a new neutrino generator for WIMP dark matter*, in *APS April meeting abstracts*, https://meetings.aps.org/Meeting/APR21/Session/SP01.6 (2021).

[30] ATLAS collaboration, *Measurements of Higgs boson production by gluon-gluon fusion and vector-boson fusion using $H \to WW^* \to e\nu\mu\nu$ decays in pp collisions at $\sqrt{s} = 13$ TeV with the ATLAS detector*, *Phys. Rev. D* **108** (2023) 032005 [arXiv:2207.00338] [INSPIRE].

[31] ATLAS collaboration, *Fiducial and differential cross-section measurements for the vector-boson-fusion production of the Higgs boson in the $H \to WW^* \to e\nu\mu\nu$ decay channel at 13 TeV with the ATLAS detector*, *Phys. Rev. D* **108** (2023) 072003 [arXiv:2304.03053] [INSPIRE].

[32] ATLAS collaboration, *Combination of searches for invisible decays of the Higgs boson using 139 fb^{-1} of proton-proton collision data at $\sqrt{s} = 13$ TeV collected with the ATLAS experiment*, *Phys. Lett. B* **842** (2023) 137963 [arXiv:2301.10731] [INSPIRE].

[33] ATLAS collaboration, *Search for dark matter produced in association with a Higgs boson decaying to tau leptons at $\sqrt{s} = 13$ TeV with the ATLAS detector*, *JHEP* **09** (2023) 189 [arXiv:2305.12938] [INSPIRE].

[34] IceCube collaboration, *Search for neutrino lines from dark matter annihilation and decay with IceCube*, arXiv:2303.13663 [INSPIRE].

[35] CMS collaboration, *A portrait of the Higgs boson by the CMS experiment ten years after the discovery*, *Nature* **607** (2022) 60 [arXiv:2207.00043] [INSPIRE].

[36] HAWC collaboration, *Discovery of gamma rays from the quiescent sun with HAWC*, *Phys. Rev. Lett.* **131** (2023) 051201 [arXiv:2212.00815] [INSPIRE].

[37] T. Linden et al., *Evidence for a new component of high-energy solar gamma-ray production*, *Phys. Rev. Lett.* **121** (2018) 131103 [arXiv:1803.05436] [INSPIRE].

[38] P. Lipari, *Lepton spectra in the earth's atmosphere*, *Astropart. Phys.* **1** (1993) 195 [INSPIRE].

[39] M. Gutiérrez, G. Hernández-Tomé, J.I. Illana and M. Masip, *Neutrino events within muon bundles at neutrino telescopes*, *Astropart. Phys.* **134-135** (2022) 102646 [arXiv:2106.01212] [INSPIRE].